

ARTICLE OPEN



El Niño phase transition by deforestation in the Maritime Continent

Shengbiao Wei^{1,2}, Xin Wang^{1,3}, Chunzai Wang^{1,3} and Qiang Xie^{4,5,6}

El Niño–Southern Oscillation (ENSO), an irregular alternation between warm El Niño and cold La Niña phases, is the most prominent air–sea interaction phenomenon on Earth and greatly affects global weather and climate. Nevertheless, it remains unclear whether human activity can alter the characteristics of ENSO. We demonstrate, using reanalysis data and coupled general circulation models, that deforestation over the Maritime Continent (MC) favors a rapid transition of El Niño to La Niña. Deforestation over the MC can induce a regional enhancement in precipitation, which in turn leads to the strengthening of the easterly trade winds over the western equatorial Pacific owing to the Gill–response. These stronger trade winds, by inducing a shoaled thermocline in the eastern Pacific, are favorable for the development of cold sea surface temperature anomalies in the eastern equatorial Pacific during El Niño decaying years. Our results suggest that El Niño is more likely to be followed by La Niña if MC deforestation continues in the future.

npj Climate and Atmospheric Science (2024)7:3; <https://doi.org/10.1038/s41612-023-00548-3>

INTRODUCTION

El Niño–Southern Oscillation (ENSO) is the strongest interannual climate variability with great global impacts^{1–4}. It is characterized by an irregular swing between El Niño and La Niña, which are respectively warmer and colder than normal sea surface temperature (SST) over the eastern and central tropical Pacific. Several conceptual theories have been proposed to explain the phase transition of ENSO, including the delayed oscillator^{5,6}, the recharge oscillator⁷, the western Pacific oscillator^{8,9}, the advective–reflective oscillator¹⁰ and the unified oscillator¹¹. In recent decades, more El Niño events have tended to turn into La Niña events (Fig. 1a). The proportion of El Niño events with a phase transition, defined here as the percentage of the number of El Niño events followed by La Niña events in the total number of El Niño events in sliding 25 years (see Methods), has prominently increased from approximately 40% before 1980 to about 70% in the latest decade (Fig. 1a, Supplementary Fig. 1, Supplementary Note 1). Explaining this increase in the number of El Niño events followed by La Niña events in recent decades is still an open issue.

Deforestation has profound impacts on the climate and environment¹². During recent decades, forests in the Maritime Continent (MC) region (10°S–10°N, 95°E–130°E) have experienced a high rate of clearing due to pressure from the local population and economy^{13–16}. Gaveau et al. (ref¹⁵) estimated that 75.7% of Borneo's area was forested around 1973 and that value had declined by 30.2% in 2010. According to forest assessment data from the United Nations Food and Agricultural Organization's (UNFAO) Forest Resource Assessment in 1990 and 2015 (ref^{17–20}), the forest cover in Indonesia experienced a monotonous decrease during 1980–2015, from 72.4% in 1980 to 52.9% in 2015 (Fig. 1a). From the Moderate Resolution Imaging Spectroradiometer (MODIS) land cover type product, the forest cover over the MC

has gradually decreased since 2001 (Fig. 1b). MC deforestation not only alters the local climate^{21–25}, but may also influences large-scale atmospheric circulation patterns^{23,24,26,27}. It is suggested that the change in the Walker circulation associated with MC deforestation is comparable to that induced by La Niña²⁴. MC deforestation may even influence on ENSO diversity, including the spatial pattern, temporal evolution, and amplitude variation²⁸. These previous results indicate possible impacts of MC deforestation on ENSO. Since the increase in the proportion of El Niño events turning into La Niña events in recent decades was occurring under MC deforestation (Fig. 1a), a hypothesis is proposed that the increase in the number of El Niño events turning into La Niña events in recent decades is partly attributed to MC deforestation.

RESULTS

The keys to the transition from El Niño to La Niña

The key features associated with the phase transition of El Niño are assessed first. For convenience, an El Niño that is followed by a La Niña is referred to as El Niño–La Niña (EN–LN), while the remainder of the El Niño events, which are followed by the neutral state, are defined as El Niño–Neutral (EN–Neutral). The composite evolutions of the Niño 3.4 index during EN–LN and EN–Neutral are compared. Here, the Niño 3.4 index is defined as the SST anomalies averaged over (5°S–5°N, 170°W–120°W), which is a widely used index for ENSO. During the developing year and the early decaying year of El Niño, the changes in the Niño 3.4 index for EN–LN and EN–Neutral are similar except in amplitude, with the warm SST anomalies developing from late spring, reaching peaks in winter, and beginning to decay in the next earlier spring (Fig. 2a). However, distinct differences in the Niño 3.4 index for EN–LN and EN–Neutral are shown during decaying summer. In EN–LN, the Niño 3.4 index

¹State Key Laboratory of Tropical Oceanography, South China Sea Institute of Oceanology, Chinese Academy of Sciences, Guangzhou, China. ²University of Chinese Academy of Sciences, Beijing, China. ³Global Ocean and Climate Research Center, South China Sea Institute of Oceanology, Chinese Academy of Sciences, Guangzhou, China. ⁴Institute of Deep-sea Science and Engineering, Chinese Academy of Sciences, Sanya, China. ⁵Laboratory for Regional Oceanography and Numerical Modeling, Qingdao National Laboratory for Marine Science and Technology, Qingdao, China. ⁶Center for Ocean Mega-Science, Chinese Academy of Sciences, Qingdao, China. ✉email: wangxin@scsio.ac.cn; cwang@scsio.ac.cn

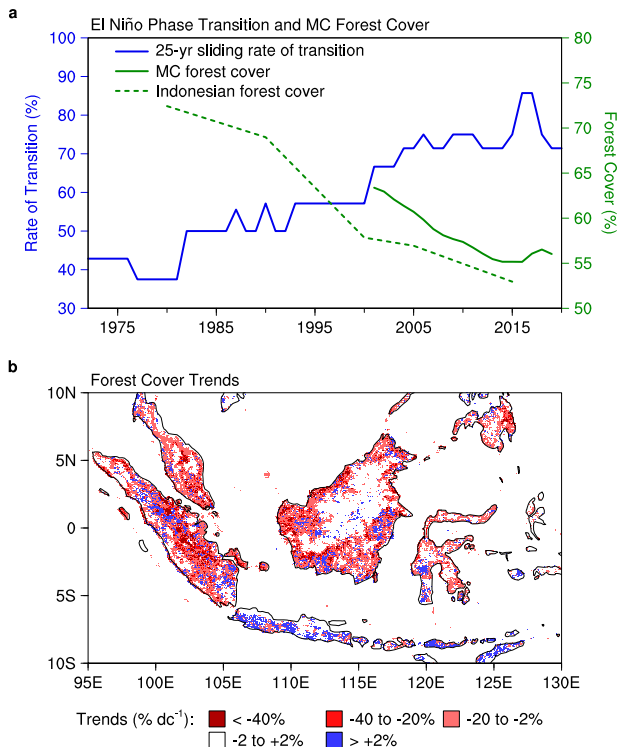


Fig. 1 Opposite changes in the forest cover over the MC and the phase transition of El Niño. **a** The 25-year sliding rate of the El Niño phase transition (%), the time series of the forest cover (%) averaged over the MC (10°S–10°N, 95°E–130°E) and the Indonesian forest cover (%). The rate of the El Niño phase transition is defined as the percentage of the number of El Niño events followed by La Niña events to the total number of El Niño events in a 25-year period (see the Methods). **b** The trends (% decade⁻¹, shading) of forest cover during 2001–2019.

indicates a rapid cooling in summer (May–June–July, MJJ), which develops into strong cold SST anomalies in the following winter. In comparison, the Niño 3.4 index in EN-Neutral decreases from the peak to neutral condition (0–0.5 °C) in May, and such a neutral Niño 3.4 index persists through winter. The timing of the phase transition of El Niño is critical and occurs in MJJ.

The differences in large-scale atmospheric circulation patterns in MJJ associated with EN-LN and EN-Neutral are examined. Compared to EN-Neutral, EN-LN features an enhanced precipitation over the MC (5°S–5°N, 100°E–125°E; red box in Fig. 2b) and anomalous lower-level easterly winds over the western equatorial Pacific (5°S–5°N, 140°E–170°W) (Fig. 2b, Supplementary Fig. 1). These circulation pattern differences are in accordance with the Gill-response²⁹, in which equatorial diabatic heating induces easterly surface wind anomalies to its east. The significant correlation coefficient as high as -0.48 ($p < 0.001$) between the anomalous MC precipitation and the zonal winds over the western Pacific (Supplementary Fig. 3a) is consistent with the dynamics of the Gill-response.

The anomalous easterly winds over the western equatorial Pacific, significantly related to the east-west thermocline tilt in the equatorial Pacific (Supplementary Fig. 3b), lead to a shoaled thermocline in the east and a deepened thermocline in the west. The shoaled thermocline in the eastern equatorial Pacific is conducive to the development of cold SST anomalies through thermocline feedback^{7,30,31} (Supplementary Fig. 4a). The significant cold SST anomalies in the eastern equatorial Pacific

can develop into La Niña in winter under the control of Bjerknes feedback. In contrast, the weaker MC precipitation in EN-Neutral is unfavorable for the emergence of cold SST anomalies (Supplementary Fig. 4b). It is clear that the phase transition of El Niño is connected with the precipitation over the MC, the more MC precipitation could favor the transition from El Niño to La Niña through inducing lower-level easterlies over the western equatorial Pacific.

The climate variations related to MC deforestation

The above results show that the precipitation over the MC and precipitation-induced lower-level easterlies over the western equatorial Pacific could be responsible for the El Niño phase transition. Based on the available observational and reanalysis data, Fig. 2c, d show close relationships of the MC forest cover with the MC precipitation and lower-level zonal wind anomalies over the western equatorial tropical Pacific, respectively. Here, the concurrent influences of the eastern Pacific SST anomalies on the precipitation and zonal wind are removed using linear regression with respect to the MJJ Niño 3.4 index. These results indicate that a reduction in the MC forest cover may lead to an enhancement in the local precipitation and stronger easterlies over the western equatorial Pacific. It is possible that these changes coincide by chance with an increase in the rate of El Niño phase transition rather than direct effects caused by MC deforestation. Therefore, in the following, the physical mechanisms behind these strong relationships are uncovered.

Deforestation in the MC can lead to local land surface warming (Supplementary Fig. 5), which is consistent with previous studies^{21,32}. Since the MC is surrounded by seas, it is suggested that land surface warming can induce stronger convergence of lower-level winds to the islands, and thus result in an increase in precipitation. To prove this, we use regional climate model (RegCM) simulations (Supplementary Fig. 6) to demonstrate the effects of deforestation on precipitation in the MC (see Supplementary Note 2). After deforestation over the MC, surface warming is seen in the islands, which induces a stronger land-sea thermal contrast and causes stronger convergence of lower-level winds towards the islands from the surrounding seas (Fig. 3a). This intensified lower-level convergence carries surplus water vapor to the islands, offsetting the local drying effect of forest clearing²⁴ and thus leading to an enhancement in precipitation (Fig. 3b). The effect is amplified in MJJ season due to the background condition of this season. The mean SST over the MC in this season is about 29 °C, which is the observed threshold for deep atmospheric convection³³.

Idealized atmospheric general circulation model (AGCM) experiments are also conducted to confirm the observed close relationship between the MC forest cover and the lower-level easterly winds over the western equatorial Pacific in Fig. 2d. More precipitation is seen over the MC when the MC forests are cleared (Fig. 4), which is consistent with the RegCM results (Fig. 3b). Note that the simulated positive precipitation anomalies are not confined to the MC region, and extend from 100°E to 150°W, which may be related to the model biases or absence of air-sea interaction in the AGCM experiments (see Supplementary Note 3). To the east of the MC, where centers of precipitation are located, easterly wind anomalies appear as a classic Gill-response to single heat source²⁹. Lower-level easterly anomalies thus prevail over the western equatorial Pacific (5°S–5°N, 140°E–170°W), similar to the observed patterns (Fig. 2b).

The simulated El Niño phase transition induced by MC deforestation

The observation and model results have provided evidence that MC deforestation can enhance local precipitation and lower-level easterly winds over the western equatorial Pacific, which

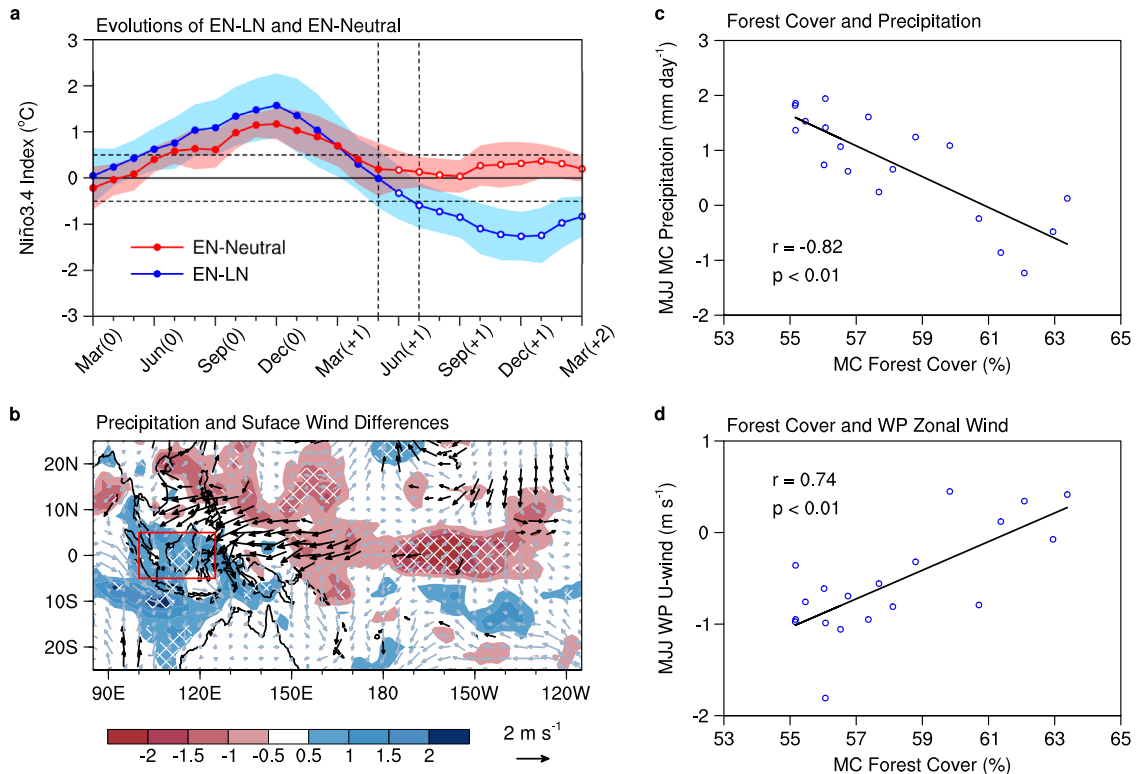


Fig. 2 Connection between the phase transition of El Niño and the MC forest cover. **a** Composite evolutions of the Niño 3.4 index ($^{\circ}\text{C}$) for EN-LN (blue line) and EN-Neutral (red line). Shading represents the ranges of ± 1 standard deviation from the mean values, and the differences between EN-LN and EN-Neutral above the 95% confidence level (Student's t -test) are marked by hollow circles. (0), (+1) and (+2) on the X-axis denote the developing, decaying and the third year of El Niño, respectively. **b** The composite differences in surface winds (m s^{-1} , vectors) and precipitation anomalies (mm day^{-1} , shading) in decaying May-June-July (MJJ) between EN-LN and EN-Neutral (EN-LN minus EN-Neutral). Darkened vectors and areas with white crosses indicate the differences in the surface winds and precipitation above the 95% confidence level (Student's t -test), respectively. **c**, **d** Scatter diagrams of the mean MC (10°S – 10°N , 95°E – 130°E , red box in **b**) and western equatorial Pacific (WP, 5°S – 5°N , 140°E – 170°W) zonal surface wind (m s^{-1}) anomalies during 2001–2019. The concurrent influences of the Niño 3.4 index on the precipitation and zonal wind have been removed using linear regression. r is the correlation coefficient, and p is the corresponding p -value. The black straight line is the linear fit.

are the key features for the transition from El Niño to La Niña. To illustrate the effect of MC deforestation on the long-term change in phase transition of El Niño, we performed two idealized model experiments (Control and Deforest runs) with coupled general circulation model (CGCM, see Methods). The CGCM experiments can simulate the EN-LN and EN-Neutral events well (Fig. 5). In both the Control and Deforest runs, the precipitation in the MC and anomalous lower-level easterly winds over the western equatorial Pacific during MJJ season are stronger in the EN-LN events than in the EN-Neutral events, similar to observations (Fig. 2b). It is also seen that the precipitation change over the MC is stronger in the Deforest run than in the Control run, consistent with the local effects of the MC deforestation. Here, the changes in the rate of El Niño phase transition (see Methods) and the differences of the Niño 3.4 index between El Niño peak season (November–December–January, NDJ) and the following NDJ season are calculated to identify the changes in the transition of El Niño (see Methods). The rate of El Niño phase transition is higher under MC deforestation, with an increase by 5.5% when MC is completely deforested (Fig. 6). The increase shows that MC deforestation is favorable for the transition from El Niño to La Niña. Furthermore, comparing the Niño 3.4 index changes between the Control and Deforest runs (Fig. 6), it is seen that the probability of Niño 3.4 index decrease more than 1.0°C is higher in the Deforest run than in the Control run, with an

increase by about 10%. The probability increase in the Deforest run also indicates that El Niño is more likely to transit to La Niña under MC deforestation. It is noteworthy that the increase in the rate of El Niño phase transition is only 5.5%, and the increase in the probability of Niño 3.4 index decrease more than 1.0°C is only about 10% under complete MC deforestation. These changes are not as prominent as those ENSO property changes due to greenhouse warming, such as the increases in extreme El Niño and La Niña frequencies^{34,35} and the changes in El Niño favor³⁶. The results show that MC deforestation only partly contributes to the change in the rate of El Niño phase transition. However, considering the small area of the MC, these increases due to MC deforestation is considerable, and deserve attention.

DISCUSSION

Our results highlight the role of MC deforestation in boosting the phase transition of El Niño (Fig. 7). Due to local surface temperature warming induced by MC deforestation, a strong land-sea thermal contrast leads to lower-level convergence of water vapor and precipitation over the MC^{37,38}. As a Gill-response of the heat released by precipitation, the lower-level easterly winds strengthen over the western equatorial Pacific. The strengthening of the lower-level easterly winds could lead to a shoaling of the thermocline over the eastern equatorial

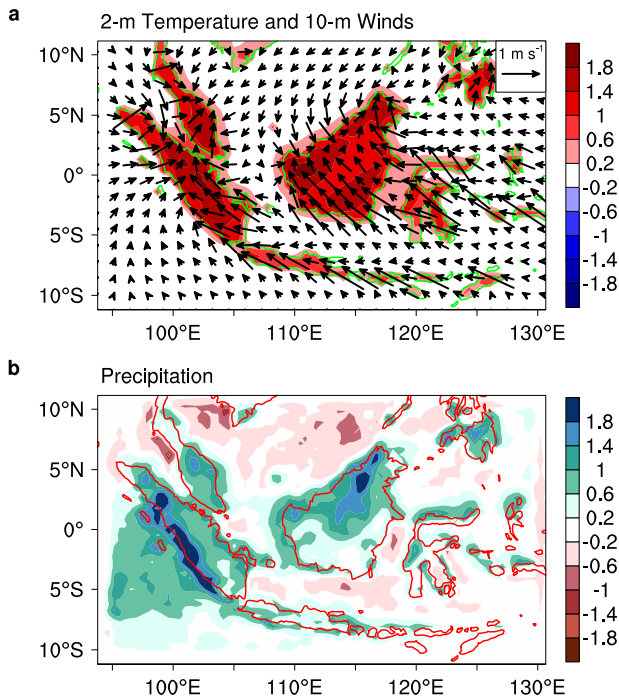


Fig. 3 Influences of MC deforestation on the local temperature and precipitation during MJJ season in RegCM experiments. **a** The differences in 2-m temperature ($^{\circ}\text{C}$, shading) and 10-m winds (m s^{-1} , vectors) during May–June–July (MJJ) between the Def-run and Ctrl-run experiments (Def-run minus Ctrl-run). **b** The differences in precipitation (mm day^{-1} , shading) between the Def-run and Ctrl-run experiments (Def-run minus Ctrl-run).

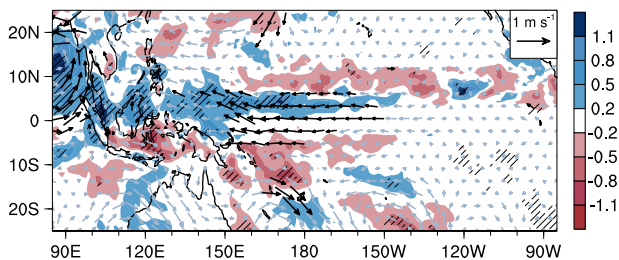


Fig. 4 Influences of MC deforestation on MJJ precipitation and 850 hPa winds in AGCM experiments. The differences in precipitation (mm day^{-1} , shadings) and 850 hPa winds (m s^{-1} , vectors) May–June–July (MJJ) between the Def-run and Ctrl-run (Def-run minus Ctrl-run). Darkened vectors and dashed areas denote the differences in the surface winds and precipitation above the 95% confidence level.

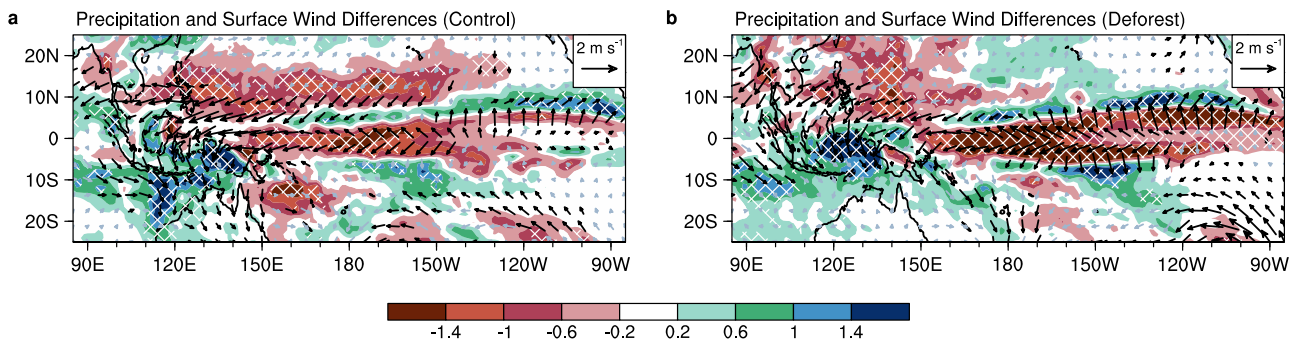


Fig. 5 ENSO pattern changes in the CGCM simulation in the MJJ season. Differences in precipitation (mm day^{-1} , shading) and surface winds (m s^{-1} , vectors) during May–June–July (MJJ) between the EN-LN and EN-Neutral (EN-LN minus EN-Neutral) in the Control **a** and Deforest **b** experiments. Darkened vectors and areas with white crosses indicate the differences in the surface winds and precipitation above the 95% confidence level (Student's *t*-test), respectively.

Pacific^{7,30}, which is critical for the cooling of the SST over the eastern equatorial Pacific due to a more efficient Bjerknes feedback. Therefore, during continuous MC deforestation in the recent decades, El Niño tends to change into La Niña, and the proportion of the El Niño with a phase transition increases (Fig. 1a). If deforestation in the MC continues in the future, the phase transition of El Niño may be more predictable, meaning that El Niño will be more likely to be followed by La Niña. In addition to the phase transition of El Niño, MC deforestation may influence other properties of ENSO. For example, the strengthening of the easterly trade winds over the western equatorial Pacific associated with MC deforestation may favor the development of La Niña, or multi-year La Niña²⁸. Such potential influence of MC deforestation is still an open study.

Many previous studies have shown that ENSO variability is influenced by greenhouse warming^{34,39–41}. Being regarded as the lungs of Earth, forests are capable of absorbing carbon dioxide via photosynthesis. Thus, deforestation can exacerbate greenhouse warming⁴² and, in this way, indirectly impact ENSO variability and hence global climate. However, our results show that deforestation in the MC can directly affect the phase transition of El Niño by changing the large-scale atmospheric circulation patterns. This finding is different from the traditional understanding of the climate impacts of deforestation. Our present study provides a new perspective on how deforestation may influence global climate, which deserves attention and further study in the future.

METHODS

Definitions of EN-LN and EN-Neutral events

In this study, the Niño 3.4 index, which is defined as the SST anomalies averaged over (5°S – 5°N , 170°W – 120°W), is used to define El Niño/La Niña. An El Niño (La Niña) is defined when the 3-month running mean Niño 3.4 index above 0.5°C (below -0.5°C) for at least 5 consecutive months. To investigate the variation in the phase transition of El Niño, we classify El Niño into El Niño–La Niña (EN-LN) and El Niño–Neutral (EN-Neutral). The EN-LN is El Niño followed by an immediate La Niña in the El Niño decaying winter, while EN-Neutral is El Niño followed by a neutral state. During 1948–2020, there were 11 EN-LN cases (1963/1964, 1969/1970, 1972/1973, 1982/1983, 1986/1987/1988, 1994/1995, 1997/1998, 2004/2005, 2006/2007, 2009/2010 and 2015/2016), and 9 EN-Neutral cases (1951/1952, 1957/1958, 1965/1966, 1968/1969, 1976/1977, 1977/1978, 1991/1992, 2002/2003 and 2018/2019). All the anomalies are calculated relative to the 1981–2010 climatology.

The MC region

The MC generally refers to the region (10°S–10°N, 95°E–130°E) in this study. When precipitation is considered, a narrower region (5°S–5°N, 100°E–125°E) is referred.

Rate of the El Niño Phase transition

This rate is defined as the percentage of the number of EN-LN cases in the number of total El Niño cases in a preceding 25-year

window. For example, the value in 2000 is calculated by the ratio during 1976–2000.

The CGCM

The CGCM used in this study is Community Earth System Model 1.2.2 (CESM) with a fully coupled component set and a 1-degree grid. In the fully coupled component set of CESM, the Community Atmosphere Model version 4 (CAM4), the Community Land Model version 4.0 (CLM4.0) with satellite phenology, the Parallel Ocean Program version 2.1 (POP2), the Community Ice CodE (CICE), and the River Transport Model (RTM) are coupled through the CESM coupler version 7 (CPL7). The model is integrated over 200 years with the state of forest cover in 2000 as spin-up, and then two idealized experiments are carried out to investigate the effects of MC deforestation on the phase transition of El Niño. In the Control run, the forests in the MC are set to the state in 2000; while in the Deforest run, all the forests in the MC are cleared, and are replaced with broadleaf evergreen trees and broadleaf deciduous trees with C4 grasses (tropical grasses). Both the Control and Deforest experiments are branched from the end of the 200-year free run of spin-up, and integrated forward for 200 years. The differences between the Control and Deforest experiments are then compared. To identify the changes in El Niño phase transition, the rates of phase transition in the two experiments are calculated. The definitions of El Niño and La Niña events are the same as in observations. Similar to the El Niño case 1986/1987/1988, warming lasting more than 2 years without a break is treated as one El Niño event in CGCM simulations. Also, the difference in Niño 3.4 index between El Niño peak season (November–December–January, NDJ) and the following NDJ season is calculated (the following NDJ minus peak NDJ). The probability of Niño 3.4 index decrease of more than 1.0 °C is compared between the Control and Deforest experiments to show the influence of MC deforestation on the phase transition of El Niño.

Statistical tests

Unless explicitly mentioned, all statistical tests are determined based on the two-tailed Student's *t*-test.

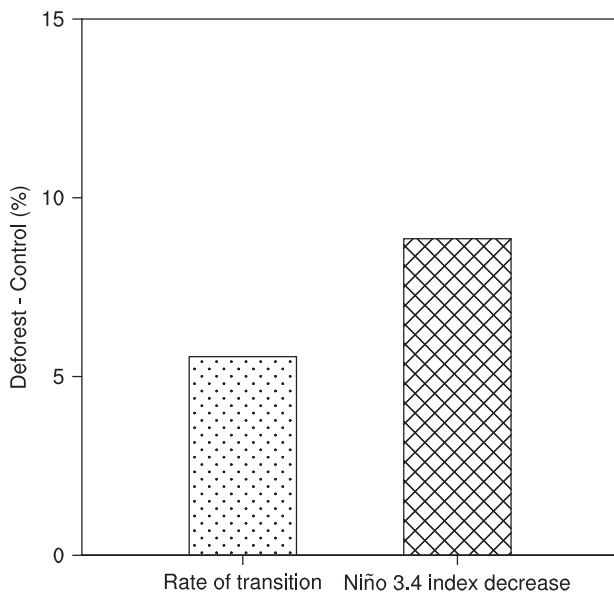


Fig. 6 Changes in El Niño properties under MC deforestation in CGCM simulations. Change in the rate (%; dotted bar) of El Niño phase transition (Deforest – Control), and Change in the probability (%; cross bar) of NDJ Niño 3.4 index decrease of more than 1.0 °C between El Niño year and the following year (Deforest – Control).

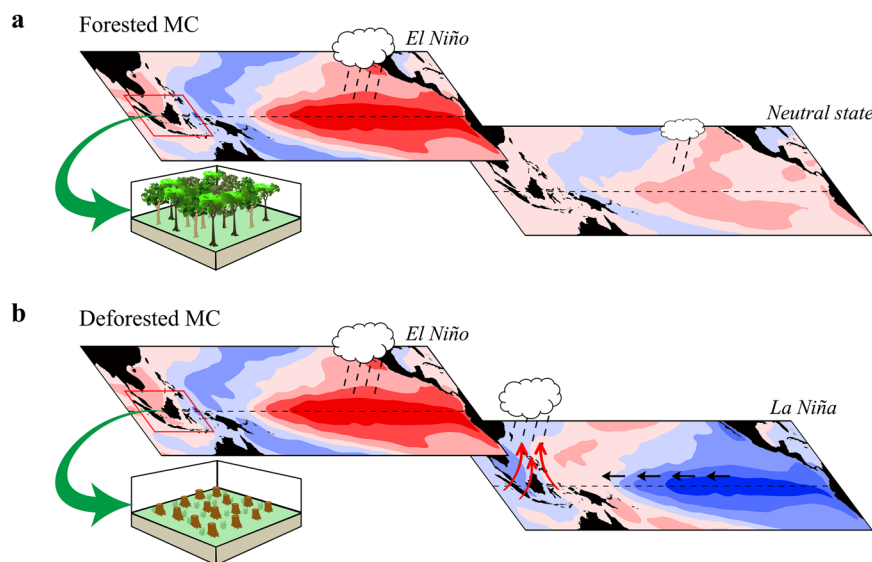


Fig. 7 Schematic depicting the influence of MC deforestation on the phase transition of El Niño. **a** The phase transition of El Niño under a forested MC. **b** The phase transition of El Niño under a deforested MC. Under a forested MC, El Niño is likely to remain in a neutral state **a** in the winter of the El Niño decaying year. When the MC is deforested, El Niño tends to turn into a La Niña state **b** due to deforestation-induced local precipitation enhancement (by inducing stronger local convergence and convection, indicated by red arrows) and the resultant anomalous western equatorial Pacific zonal winds (indicated by black arrows). The symbols of tree, stump, and grass courtesy of the Integration and Application Network (<https://ian.umces.edu/media-library/>), license <https://creativecommons.org/licenses/by-sa/4.0/>).

DATA AVAILABILITY

The monthly sea surface temperature during 1948–2020 is from the Hadley Centre Sea Ice and Sea Surface Temperature⁴³ (HadISST) dataset (<https://www.metoffice.gov.uk/hadobs/hadisst/>). The monthly surface winds and precipitation during 1948–2020 are from the National Center for Environmental Prediction (NCEP) and National Center for Atmospheric Research (NCAR) reanalysis data⁴⁴ (<https://psl.noaa.gov/data/gridded/data.ncep.reanalysis.html>). The yearly land cover type data during 2001–2019 are from the Moderate Resolution Imaging Spectroradiometer (MODIS) MCD12C1 product (<https://lpdaac.usgs.gov/products/mcd12c1v006/>). The forests in the MC are represented by a combination of evergreen broadleaf forests and deciduous broadleaf forests that are based on the leaf area index (LAI) classification. In addition, country-based forest extent assessment data from the United Nations Food and Agricultural Organization's Forest Resource Assessment (UNFAO-FRA) in 1990 and 2015 are also used^{17–20} (<http://www.fao.org/forest-resources-assessment/>). The Indonesian forest extent in 1980 is inferred from the annual deforestation and plantation rates during 1980–1990 from UNFAO-FRA 1990, and those in 1990, 2000, 2005, 2010, and 2015 are from UNFAO-FRA 2015. RegCM, CAM4, and CESM simulated data are available at <https://data.scio.ac.cn/metaData-detail/1731888315977166848>, or on request from the corresponding authors.

CODE AVAILABILITY

All analyses were performed using NCAR Command Language (NCL). The codes for calculations are available at <https://pan.cstcloud.cn/s/48A8UWP9T9A> or on request from the corresponding authors.

Received: 26 May 2023; Accepted: 11 December 2023;

Published online: 02 January 2024

REFERENCES

- Ropelewski, C. F. & Halpert, M. S. Global and regional scale precipitation patterns associated with the El Niño/Southern Oscillation. *Mon. Weath. Rev.* **115**, 1606–1626 (1987).
- McPhaden, M. J., Zebiak, S. E. & Glantz, M. H. ENSO as an integrating concept in Earth science. *Science* **314**, 1740–1745 (2006).
- Yeh, S.-W. et al. ENSO atmospheric tel-econnections and their response to greenhouse gas forcing. *Rev. Geophys.* **56**, 185–206 (2018).
- Taschetto, A. S. et al. ENSO atmospheric teleconnections. *El Niño Southern Oscillation in a Changing Climate* (pp. 309–335). American Geophysical Union (AGU) (2020).
- Suarez, M. J. & Schopf, P. S. A delayed action oscillator for ENSO. *J. Atmos. Sci.* **45**, 3283–3287 (1988).
- Battisti, D. S. & Hirst, A. C. Interannual variability in a tropical atmosphere ocean model-influence of the basic state, ocean geometry and nonlinearity. *J. Atmos. Sci.* **46**, 1687–1712 (1989).
- Jin, F.-F. An equatorial ocean recharge paradigm for ENSO. Part I: Conceptual model. *J. Atmos. Sci.* **54**, 811–829 (1997).
- Weisberg, R. H. & Wang, C. A western Pacific oscillator paradigm for the El Niño-Southern Oscillation. *Geophys. Res. Lett.* **24**, 779–782 (1997).
- Wang, C., Weisberg, R. H. & Virmani, J. I. Western Pacific interannual variability associated with the El Niño-Southern Oscillation. *J. Geophys. Res.* **104**, 5131–5149 (1999).
- Picaut, J., Masia, F. & duPenhoat, Y. An advective-reflective conceptual model for the oscillatory nature of the ENSO. *Science* **277**, 663–666 (1997).
- Wang, C. A unified oscillator model for the El Niño-Southern Oscillation. *J. Clim.* **14**, 98–115 (2001).
- Bonan, G. B. Forests and climate change: Forcings, feedbacks, and the climate benefits of forests. *Science* **320**, 1444–1449 (2008).
- Margono, B. A. et al. Mapping and monitoring deforestation and forest degradation in Sumatra (Indonesia) using Landsat time series data sets from 1990 to 2010. *Environ. Res. Lett.* **7**, 034010 (2012).
- Hansen, M. C. et al. High-resolution global maps of 21st-century forest cover change. *Science* **342**, 850–853 (2013).
- Gaveau, D. L. A. et al. Four decades of forest persistence, clearance and logging on Borneo. *PLoS ONE* **9**, e101654 (2014).
- Margono, B. A., Potapov, P. V., Turubanova, S., Stolle, F. & Hansen, M. C. Primary forest cover loss in Indonesia over 2000–2012. *Nat. Clim. Chang.* **4**, 730–735 (2014).
- FAO (Food and Agriculture Organization) *Forest Resources Assessment 1990 Global Synthesis*. FAO Forestry Paper 124 (UNFAO, Rome), (1995).
- FAO (Food and Agriculture Organization) *Forest Resources Assessment 1990 Tropical countries*. FAO Forestry Paper 112 (UNFAO, Rome), (1993).
- FAO (Food and Agriculture Organization) *Global Forest Resources Assessment 2015 Desk reference*. (UNFAO, Rome), (2015).
- FAO (Food and Agriculture Organization) *Global Forest Resource Assessment 2015 Country Report: Indonesia*. (UNFAO, Rome), (2014).
- Li, Y. et al. Local cooling and warming effects of forests based on satellite observations. *Nat. Commun.* **6**, 6603 (2015).
- Alkama, R. & Cescatti, A. Biophysical climate impacts of recent changes in global forest cover. *Science* **351**, 600–604 (2016).
- Schneck, R. & Mosbrugger, V. Simulated climate effects of Southeast Asian deforestation: regional processes and teleconnection mechanisms. *J. Geophys. Res.* **116**, D11116 (2011).
- Chen, C.-C. et al. Thermodynamic and dynamic responses to deforestation in the Maritime Continent: a modeling study. *J. Clim.* **32**, 3505–3527 (2019).
- Lee, T.-H. & Lo, M.-H. The role of El Niño in modulating the effects of deforestation in the Maritime Continent. *Environ. Res. Lett.* **16**, 054056 (2021).
- Wei, S., Wang, X. & Xie, Q. Strengthening effect of Maritime Continent deforestation on the precipitation decline over southern China during late winter and early spring. *Clim. Dyn.* **60**, 1173–1185 (2023).
- Mabuchi, K., Sato, Y. & Kida, H. Climatic impact of vegetation change in the Asian tropical region. Part I: Case of the northern hemisphere summer. *J. Clim.* **18**, 410–428 (2005).
- Lee, T.-H., Yu, J.-Y., Lin, Y.-F., Lo, M.-H. & Xiao, H.-M. The potential influence of maritime continent deforestation on El Niño-Southern Oscillation: Insights from idealized modeling experiments. *Geophys. Res. Lett.* **50**, e2023GL105012 (2023).
- Gill, A. E. Some simple solutions for heat-induced tropical circulation. *Quart. J. Meteorol. Soc.* **106**, 447–462 (1980).
- Jin, F.-F. & An, S.-I. Thermocline and zonal advective feedbacks within the equatorial ocean recharge oscillator model for ENSO. *Geophys. Res. Lett.* **26**, 2989–2992 (1999).
- Jin, F.-F., Kim, S. T. & Bejarano, L. A coupled-stability index for ENSO. *Geophys. Res. Lett.* **33**, L23708 (2006).
- Davin, E. L. & de Noblet-Ducoudre, N. Climatic impact of global-scale deforestation: Radiative versus nonradiative processes. *J. Clim.* **23**, 97–112 (2010).
- Xie, R., Mu, M. & Fang, X. New indices for better understanding ENSO by incorporating convection sensitivity to sea surface temperature. *J. Clim.* **33**, 7045–7061 (2020).
- Cai, W. et al. ENSO and greenhouse warming. *Nat. Clim. Chang.* **5**, 849–859 (2015).
- Cai, W. et al. Increased frequency of extreme La Niña events under greenhouse warming. *Nat. Clim. Chang.* **5**, 132–137 (2015).
- Yeh, S.-W. et al. El Niño in a changing climate. *Nature* **461**, 511–514 (2009).
- Qian, J.-H. Why precipitation is mostly concentrated over islands in the Maritime Continent. *J. Atmos. Sci.* **65**, 1428–1441 (2008).
- Ruppert, J. H. & Chen, X. Island precipitation enhancement in the Maritime Continent. *Geophys. Res. Lett.* **47**, e2019GL086545 (2020).
- Fredriksen, H.-B., Berner, J., Subramanian, A. C. & Capotondi, A. How does El Niño-Southern Oscillation change under global warming—A first look at CMIP6. *Geophys. Res. Lett.* **47**, e2020GL090640 (2020).
- Berner, J., Christensen, H. M. & Sardeshmukh, P. D. Does ENSO regularity increase in a warming climate? *J. Clim.* **33**, 1247–1259 (2020).
- Collins, M. et al. The impact of global warming on the tropical Pacific ocean and El Niño. *Nat. Geosci.* **3**, 391–397 (2010).
- Baccini, A. et al. Estimated carbon dioxide emissions from tropical deforestation improved by carbon-density maps. *Nat. Clim. Chang.* **2**, 182–185 (2012).
- Rayner, N. A. et al. Global analyses of sea surface temperature, sea ice, and night marine air temperature since the late nineteenth century. *J. Geophys. Res.* **108**, 4407 (2003).
- Kalnay, E. et al. The NCEP/NCAR 40-year reanalysis project. *Bull. Am. Meteorol. Soc.* **77**, 437–471 (1996).

ACKNOWLEDGEMENTS

This work was supported by the National Natural Science Foundation of China (Grant Nos. 41925024 and 42330404), the Strategic Priority Research Program of the Chinese Academy of Sciences (Grant No. XDB42000000), and the special fund of South China Sea Institute of Oceanology of the Chinese Academy of Sciences (SCSIO2023QY01). C.W. was supported by the National Natural Science Foundation of China (42192564), the National Key R&D Program of China (2019YFA0606701), and the development fund of the South China Sea Institute of Oceanology of the Chinese Academy of Sciences (SCSIO202208). The numerical simulation is supported by the High-Performance Computing Division at the South China Sea Institute of Oceanology.

AUTHOR CONTRIBUTIONS

X.W. conceived the study and directed the analyses. S.W. performed the data analyses and numerical experiments. X.W. and S.W. wrote the initial version of the paper. C.W. advised the research and substantively improved the paper. All authors discussed the results and helped improve the paper. S.W. and X.W. are co-first authors.

COMPETING INTERESTS

The authors declare no competing interests.

ADDITIONAL INFORMATION

Supplementary information The online version contains supplementary material available at <https://doi.org/10.1038/s41612-023-00548-3>.

Correspondence and requests for materials should be addressed to Xin Wang or Chunzai Wang.

Reprints and permission information is available at <http://www.nature.com/reprints>

Publisher's note Springer Nature remains neutral with regard to jurisdictional claims in published maps and institutional affiliations.



Open Access This article is licensed under a Creative Commons Attribution 4.0 International License, which permits use, sharing, adaptation, distribution and reproduction in any medium or format, as long as you give appropriate credit to the original author(s) and the source, provide a link to the Creative Commons license, and indicate if changes were made. The images or other third party material in this article are included in the article's Creative Commons license, unless indicated otherwise in a credit line to the material. If material is not included in the article's Creative Commons license and your intended use is not permitted by statutory regulation or exceeds the permitted use, you will need to obtain permission directly from the copyright holder. To view a copy of this license, visit <http://creativecommons.org/licenses/by/4.0/>.

© The Author(s) 2024